Supporting Information

Molecular dynamics interpretation of hydrogen bonds for colorless, water-resistant, tough, and self-healable elastomers

Seon-Mi Kim,‡[a], Minkyung Lee,‡[a], Sanggil Park,‡[b], Seul-A Park,[a] Hyeonyeol Jeon,[a] Jun Mo Koo,[a,c] Sung Bae Park,[a] Hyo Jeong Kim,[a] Youngho Eom,[a,d] Eun Seong Lee,[e] Hyungjun Kim,*[b] Dongyeop X. Oh*[a,f] and Jeyoung Park*[a,g]

[a] *Research Center for Bio-based Chemistry, Korea Research Institute of Chemical Technology (KRICT), Ulsan 44429, Republic of Korea*
[b] *Department of Chemistry and Research Institute of Basic Sciences, Incheon National University, Incheon 22012, Republic of Korea*
[c] *Department of Organic Materials Engineering, Chungnam National University, Daejeon 34134, Republic of Korea*
[d] *Department of Polymer Engineering, Pukyong National University, Busan 48513, Republic of Korea*
[e] *Department of Biomedical Chemical Engineering, The Catholic University of Korea, Bucheon, Gyeonggi-do 14662, Republic of Korea*
[f] *Department of Polymer Science and Engineering and Program in Environmental and Polymer Engineering, Inha University, Incheon 22212, Republic of Korea*
[g] *Department of Chemical and Biomolecular Engineering, Sogang University, Seoul 04107, Republic of Korea*
‡ *These authors contributed to this work equally.*

*E-mail: kim.hyungjun@inu.ac.kr, d.oh@inha.ac.kr, jeypark@sogang.ac.kr

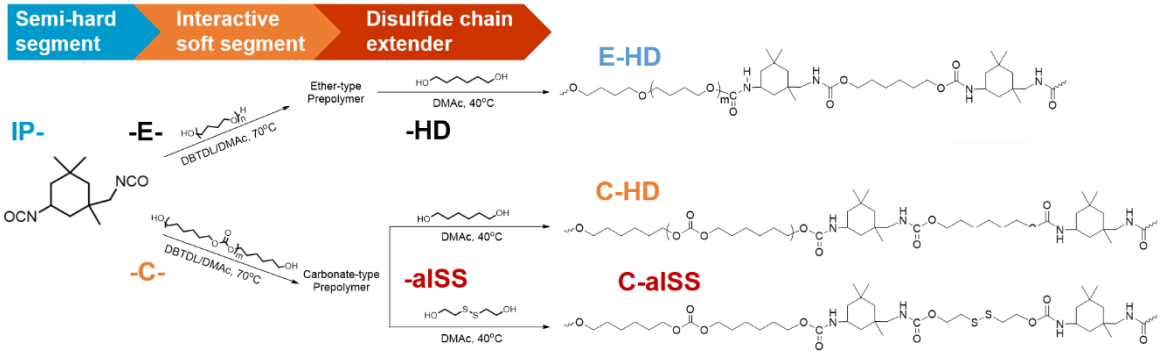

Figure S1. Synthetic route to TPUs with different soft segments and extenders. The prepared TPUs are designated as X-Y in which X and Y stand for the abbreviation of the type of macrodiol and chain extender, respectively (E-HD, C-HD, and C-alSS).

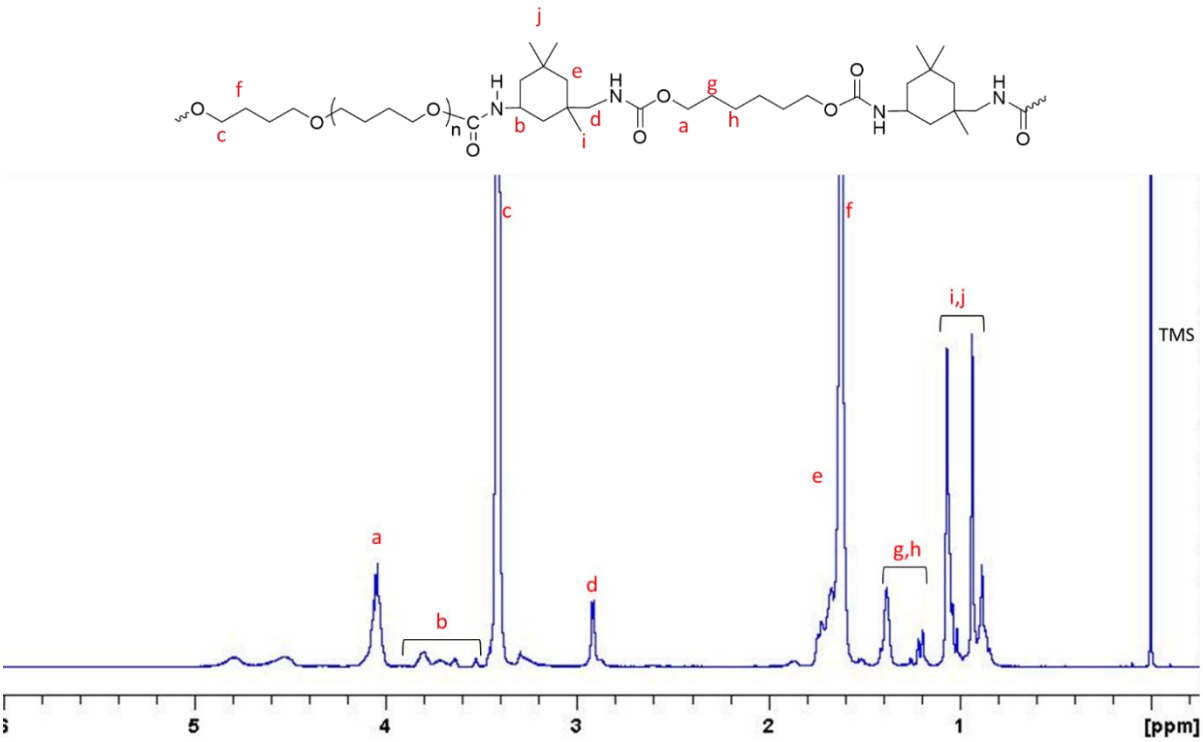

Figure S2. ^{1}H NMR spectrum of E-HD in $CDCl_3$ (600 MHz). In the ^{1}H NMR spectrum of E-HD, the peaks of HD unit appeared at 1.45~1.15 ppm, the peaks of PTMEG (E) protons appeared at 3.4 and 1.6 ppm, and the peaks of IP alkyl unit appeared at 1.15~0.8 ppm. Integral ratio of each units was well-matched with feed molar ratio.

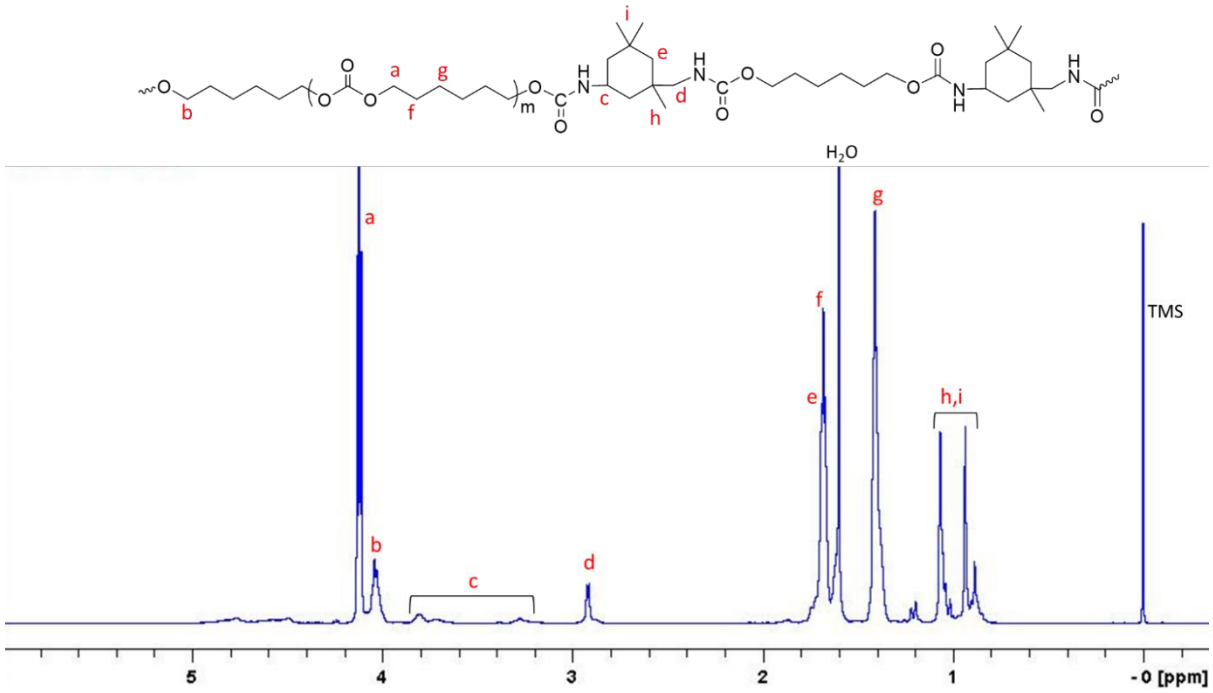

Figure S3. ^{1}H NMR spectrum of C-HD in $CDCl_3$ (600 MHz). In the ^{1}H NMR spectrum of C-HD, the peaks of protons adjacent to carbonate group of poly(hexamethylene carbonate) diol (C) appeared at 4.2~4.0 ppm, and the peaks of IP alkyl unit appeared at 1.15~0.8 ppm. Integral ratio of each units was well-matched with feed molar ratio.

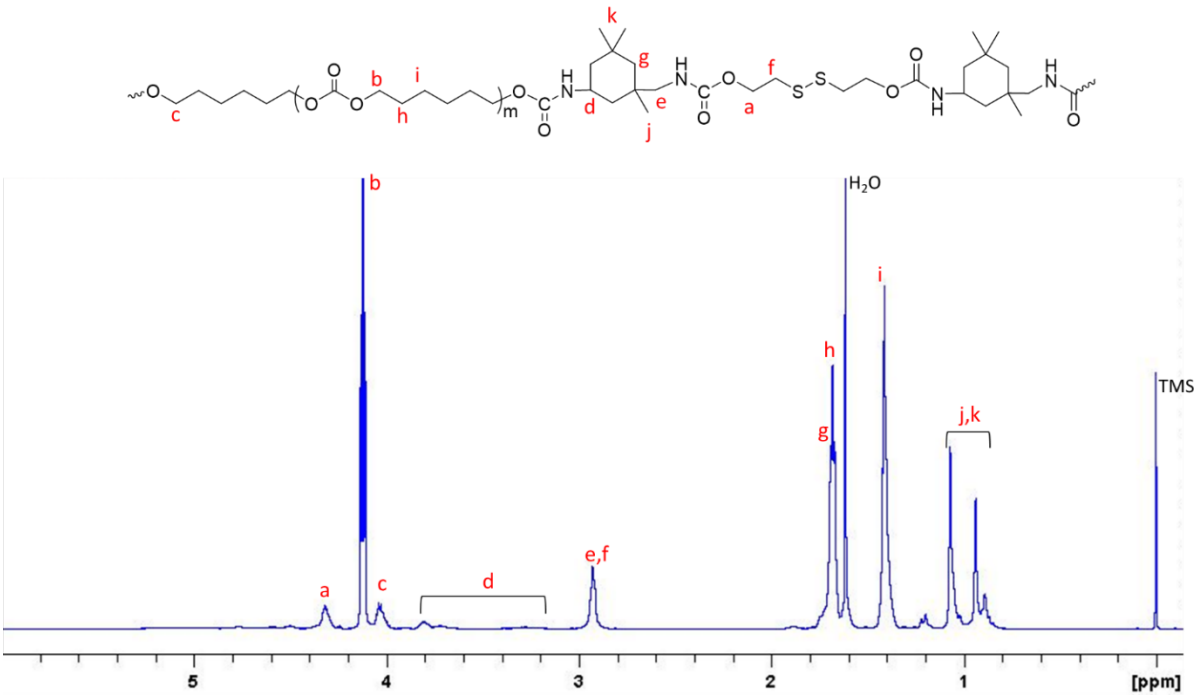

Figure S4. ^{1}H NMR spectrum of C-alSS in $CDCl_3$ (600 MHz). In the ^{1}H NMR spectrum of C-alSS, the peaks of alSS aliphatic unit appeared at 4.3 and 2.9 ppm, the peaks of protons adjacent to carbonate group of poly(hexamethylene carbonate) diol (C) appeared at 4.2~4.0 ppm, and the peaks of IP alkyl unit appeared at 1.15~0.8 ppm. Integral ratio of each units was well-matched with feed molar ratio.

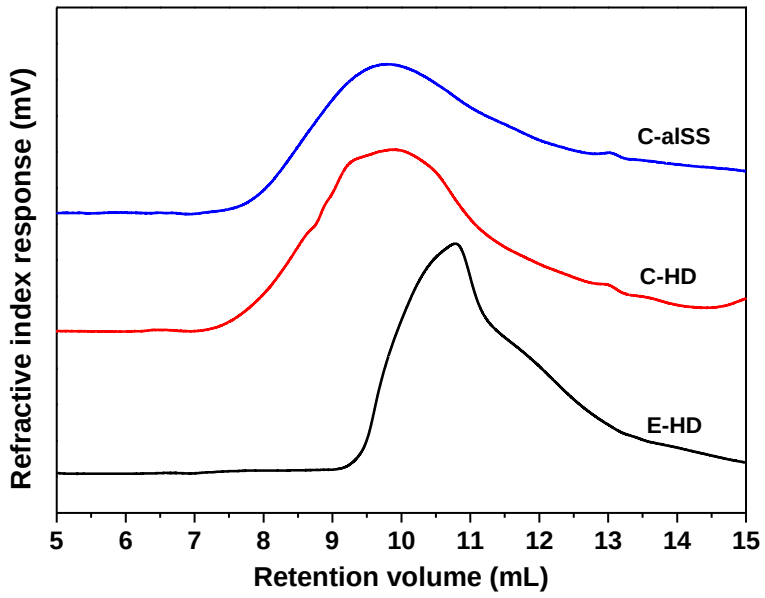

Figure S5. Chloroform-gel permeation chromatography (GPC) profiles of the synthesized TPUs.

Table S1. Polymer information and polymerization results

Entry[a)]	Content of hard segment[b)] (wt%)	M_n (g mol^{-1})[c)]	M_w (g mol^{-1})[c)]	PDI[c)]
E-HD	36.0	42,500	56,900	1.34
C-HD	36.0	89,900	136,400	1.52
C-alSS	37.5	95,800	142,000	1.48

[a)]Polymers synthesized in this study were designated as *X*-*Y* where *X* and *Y* denote the abbreviation of macrodiol and chain-extender, respectively (**E**: Poly(tetramethylene ether)glycol , **C**: Poly(hexamethylene carbonate) diol, **HD**: 1,6-hexanediol, and **alSS** : 2-hydroxyethyl disulfide; isophorone diisocyanate is fixed). [b)]Based on the weight percentages of chain-extender and diisocyanate included in the total feed weight. [c)]Determined by chloroform-GPC using polystyrene standards (RI detector).

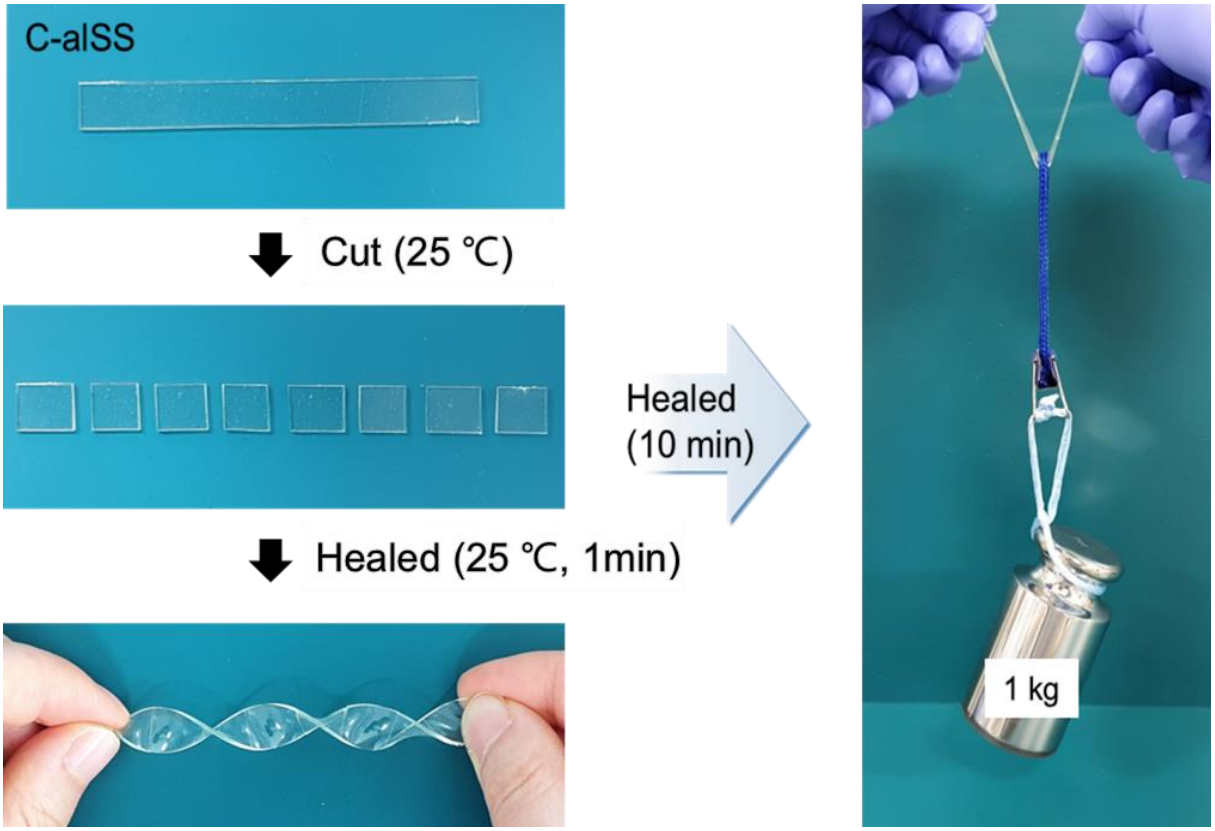

Figure S6. C-alSS of 5 mm × 1 mm was cut into five pieces and re-spliced, then recovered at room temperature (25 ℃). The film endured manual twisting and stretching after just 1 minute of recovery and withstand a 1 kg weight after 10 min.

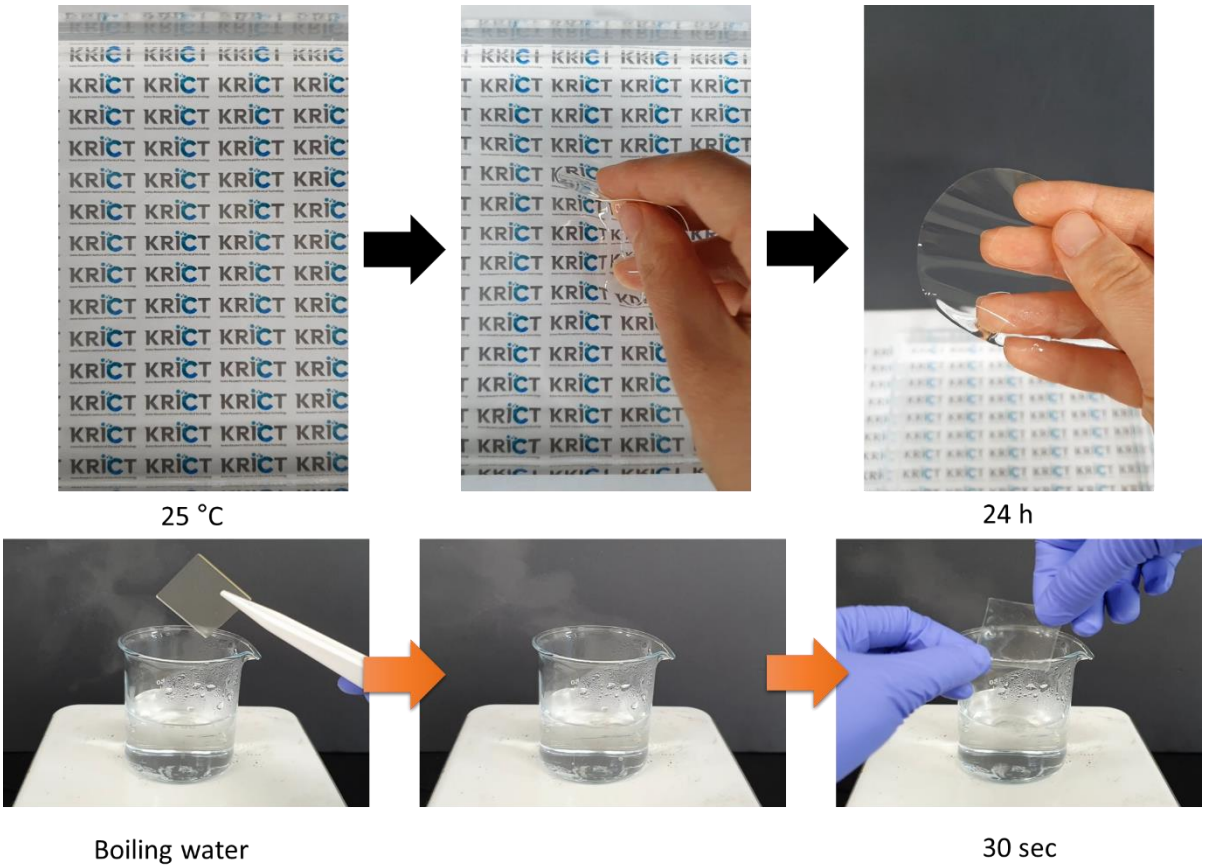

Figure S7. Water resistance of C-alSS. No dimensional change (Top) in 25 °C water for 24 h, and even after soaked (Bottom) in a boiling water for 30 s. See Movie S3 and S4.

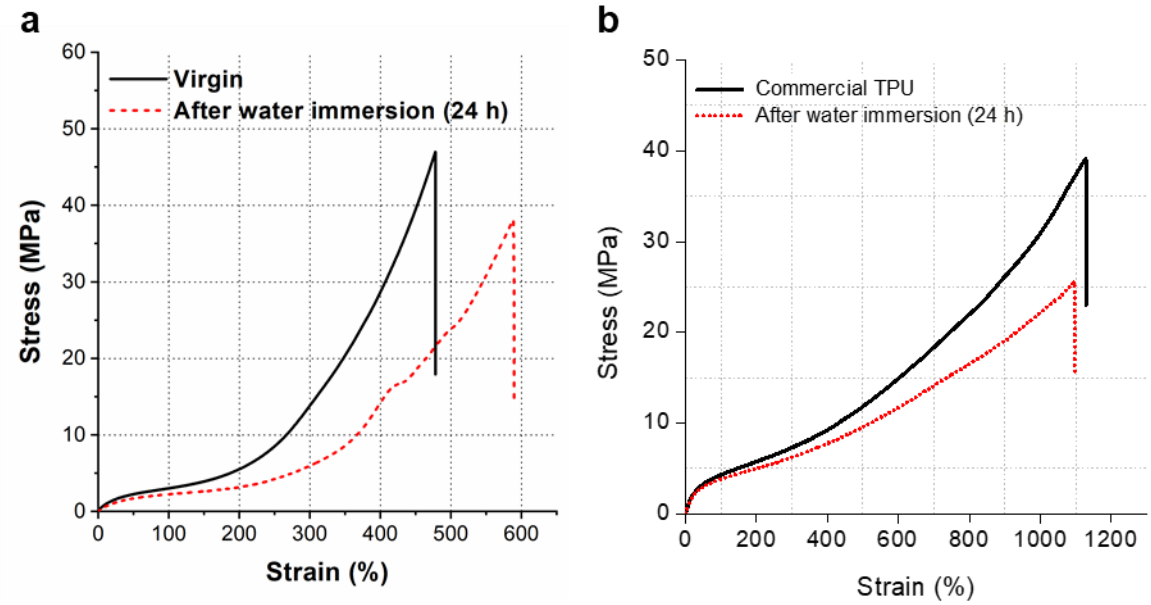

Figure S8. A comparison of stress-strain curves of a) C-alSS and b) commercial Cm-TPU before and after water immersion for 24 h.

Table S2. Information on tensile properties of a) C-alSS and b) commercial Cm-TPU before and after water immersion for 24 h.

a)

	Entry	Virgin	After immersion for 24 h under water
C-alSS	Young's modulus (MPa)	24.5 ± 1.7	16.8 ± 1.1
	UTS (MPa)	45.4 ± 1.6	33.5 ± 1.6
	Elongation at break (%)	481 ± 4	552 ± 11
	Toughness (MJ m-3)	64.6 ± 2.2	50.5 ± 3.3

b)

	Entry	Virgin	After immersion for 24 h under water
Commercial Cm-TPU	Young's modulus (MPa)	6.00 ± 0.6	3.28 ± 0.2
	UTS (MPa)	37.7 ± 1.4	24.9 ± 1.2
	Elongation at break (%)	1132 ± 7.7	1099 ± 25
	Toughness (MJ m-3)	174 ± 4.8	127 ± 9.1

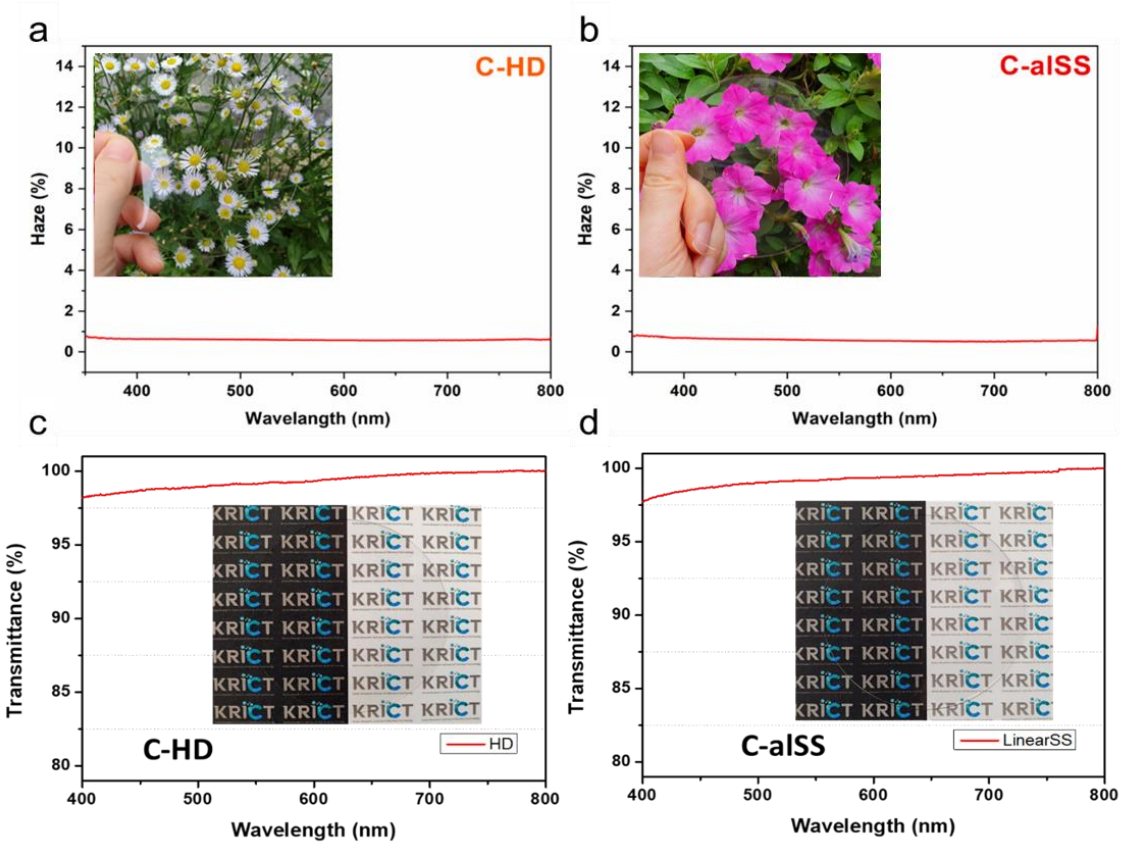

Figure S9. Haze spectrum of (a) C-HD and (b) C-alSS films. The film in the photograph was 80 mm in diameter and 0.3 mm in thickness. Photograph of (c) C-HD and (d) C-alSS. Their transmission spectrum. The film in the photograph was 80 mm in diameter and 0.3 mm in thickness.

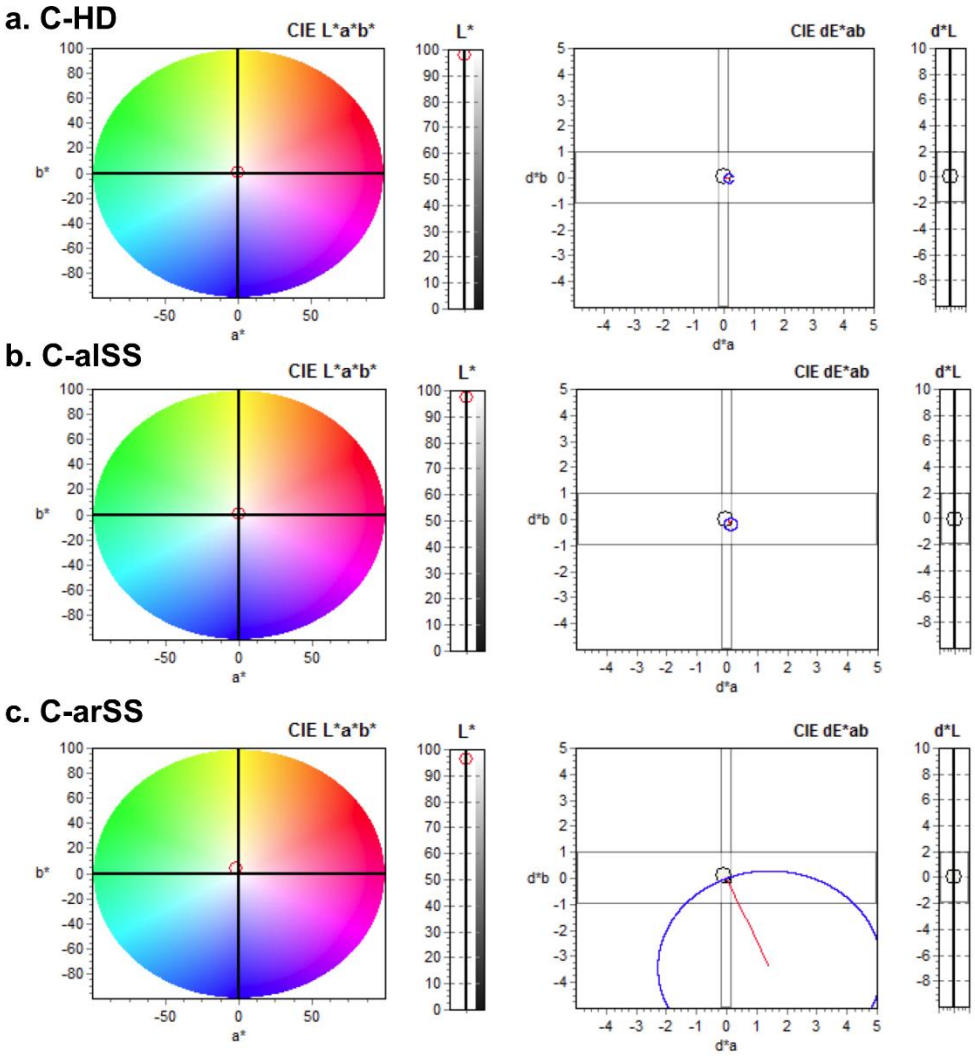

Figure S10. The CIE *L*a*b** color space and lightness (*L**) values of (a) C-HD, (b) C-alSS, and (c) C-ArSS. The *L** values of C-HD, C-alSS, and C-ArSS are 97.6, 97.5, and 96.4, respectively, and the *a*b** values of C-HD, C-alSS, and C-ArSS are (-0.12, 0.05), (-0.14, 0.15), and (-1.45, 3.49), respectively.

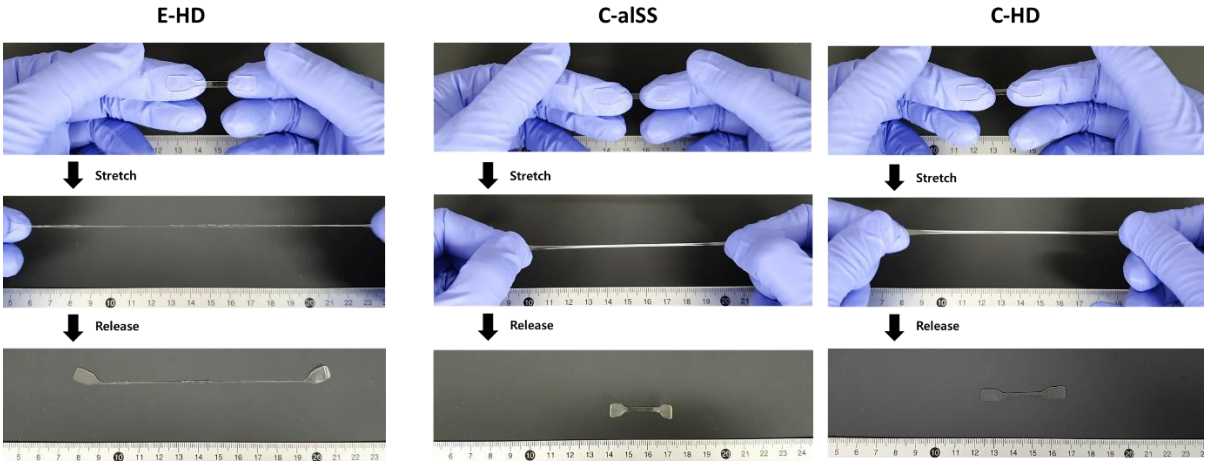

Figure S11. Photographs of dumbbell-shaped specimens of the synthesized TPUs upon stretching and after released.

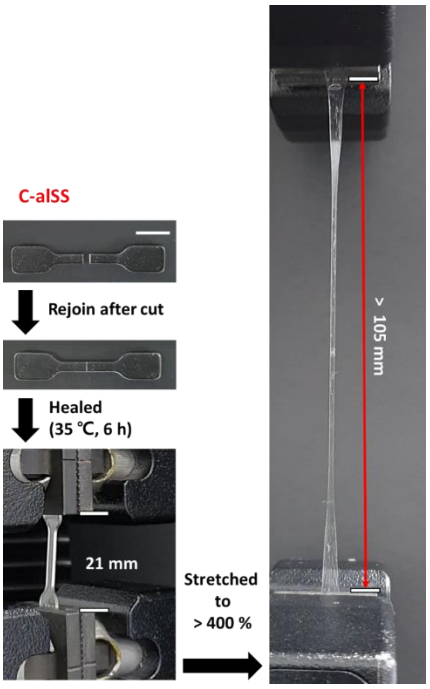

Figure S12. Photographic images of cut and healed C-alSS specimen before and after stretching up to 400% (scale bar: 1 cm).

Table S3. Information on tensile properties of TPU films and the degree of recovery after self-healing

Entry		E-HD[a)]	C-HD[b)]		C-alSS[b)]		Cm-TPU
Virgin sample	Young's modulus (MPa)	1.53 ± 0.05	31.1 ± 0.3		24.5 ± 1.7		8.86 ± 0.4
	UTS (MPa)	0.37 ± 0.001	68.4 ± 2.3		45.4 ± 1.6		35.8 ± 0.8
	Elongation at break (%)	771 ± 34	571 ± 11		481 ± 4		880 ± 8
	Toughness (MJ m^{-3})	1.14 ± 0.07	116.7 ± 6.3		64.6 ± 2.2		115 ± 2
Cut & healed sample (25−35 °C)	Young's modulus (MPa)	1.62 ± 0.08	15.5 ± 0.2	16.6 ± 0.6	22.4 ± 1.9	23.3 ± 3.1	-[c)]
	UTS (MPa)	0.39 ± 0.008	29.3 ± 0.6	31.3 ± 1.4	40.8 ± 3.0	43.7 ± 5.5	-
	Recovery of UTS (%)	105.4	42.8	45.7	89.9	96.2	-
	Elongation at break (%)	625 ± 157	394 ± 6	392 ± 11	479 ± 4.5	447 ± 18.6	-
	Recovery of elongation (%)	81.0	69.0	68.6	99.6	92.9	-
	Toughness (MJ m^{-3})	1.21 ± 0.16	41.6 ± 1.0	44.4 ± 2.5	57.0 ± 3.7	59.0 ± 9.2	-
	Recovery of toughness (%)	106.1	35.6	38.0	88.2	91.3	-

[a)]Self-healing for 2 h at 25 °C. [b)]Self-healing at 35 °C for 6 h (red color in left column) or 24 h (blue color in right column). [c)]No mechanical recovery was observed.

Table S4. Numerical value of the fragmentation energy, sulfide's H-bonding interaction, and the calculated bond dissociation energy of S-S bond (BDE_{S-S}) of alSS and ArSS. Fragmentation energy is the sum of H-bonding interaction and BDE_{S-S}.

kcal mol^{-1}	Fragmentation energy	H-bonding interaction	BDE_{S-S}
alSS	74.2	43.7	30.5
ArSS	50.8	34.2	16.6

Supporting Note 1. Details of the Quantum Chemical Simulation

Quantum chemical simulations were employed to determine the fragmentation energy required for C-alSS and ArSS to dissociate into their respective sulfide radicals (RS•). To make the simulations manageable, we simplified the structures by maintaining a single S-S bond—the repeating unit—and replacing lengthy carbon chains with methyl groups. This approach still ensured high accuracy.

For the geometry optimization of C-alSS and ArSS repeating units and their sulfide radical fragments, we utilized density functional theory (DFT). We opted for the ωB97X-D, a long-range corrected functional, based on its proven reliability in previous benchmark studies.[1] We used the 6-31G(d,p) basis set for geometry optimizations and refined single-point energies with a larger basis set, 6-311++G(d,p), as per standard recommendations.

The fragmentation energy of the polymer is defined as follows: E(repeating unit) – 2 × E(RS•) where E represents the electronic energy. The strength of both the S-S bond and the hydrogen

bonding (H-bonding) interaction within the sulfide chains are key factors in assessing the polymers' potential as self-healing materials.

We break down the fragmentation energy into two components: the bond dissociation energy of the S-S bond (BDES-S) and the H-bonding interaction of sulfide chains (refer to Table S4 in the Supporting Information). The homolytic cleavage of the S-S bond primarily results in an unpaired electron on the sulfur atoms. The structure of these polymers in triplet states is characterized by a broken S-S bond with unpaired electrons on the sulfur atoms, and remaining H-bonding interactions.

Therefore, we used the triplet state geometry to estimate $BDE_{S\text{-}S}$ as follows: E (repeating unit at the S_0 geometries) – E (repeating unit at the T_1 geometry) where S_0 and T_1 represent the singlet ground state and the first triplet state, respectively. The H-bonding interaction energy is computed by the difference between the fragmentation energy and the $BDE_{S\text{-}S}$. All calculations were performed with Q-Chem 5.2.[2]

Table S5. Tensile and self-healing properties of polymers containing disulfides.

Disulfides	Polymers[a)]	UTS (MPa)	Self-healing temperature (°C)	Recovery time (h)	UTS recovery (%)	Ref.
aliphatic	PU	~14	110	1	~80	[3]
	PUU	25	100	2	92	[4]
	PU	~20	90	24	94	[5]
	PUU	~13	80		~92	[6]
	TPU	~11		4	~91	[7]
		8.1		24	38	[8]
		3.0			84	[9]
	PU	2.2		4	~95	[10]
	PUU	~25	60	24	94	[11]
	TPU	26.3	70	0.5	~98	[12]
		25		6	86	[13]
		45	35		90	This study
	PU	7.4	25	24	98	[14]
		2.9			84	[15]
	Polysulfide	0.23			91	[16]
Aromatic	NBR	9.9	125	4	60	[17]
	PUU	11.4	40	1	~95	[18]
		18.4	37	24	75	[19]
	TPU	43	35	48	77	[20]
		6.8	25	2	88	[21]
	PUU	19		10	95	[22]
		~12		30	~90	[23]
		~9		24	100	[24]
		4.5		24	93	[25]
		4.3		48	86	[26]
		0.81		2	80	[27]
	PU	1.7		72	92	[28]

[a)] PUU: Poly(urea-urethane); NBR: Nitrile butadiene rubber.

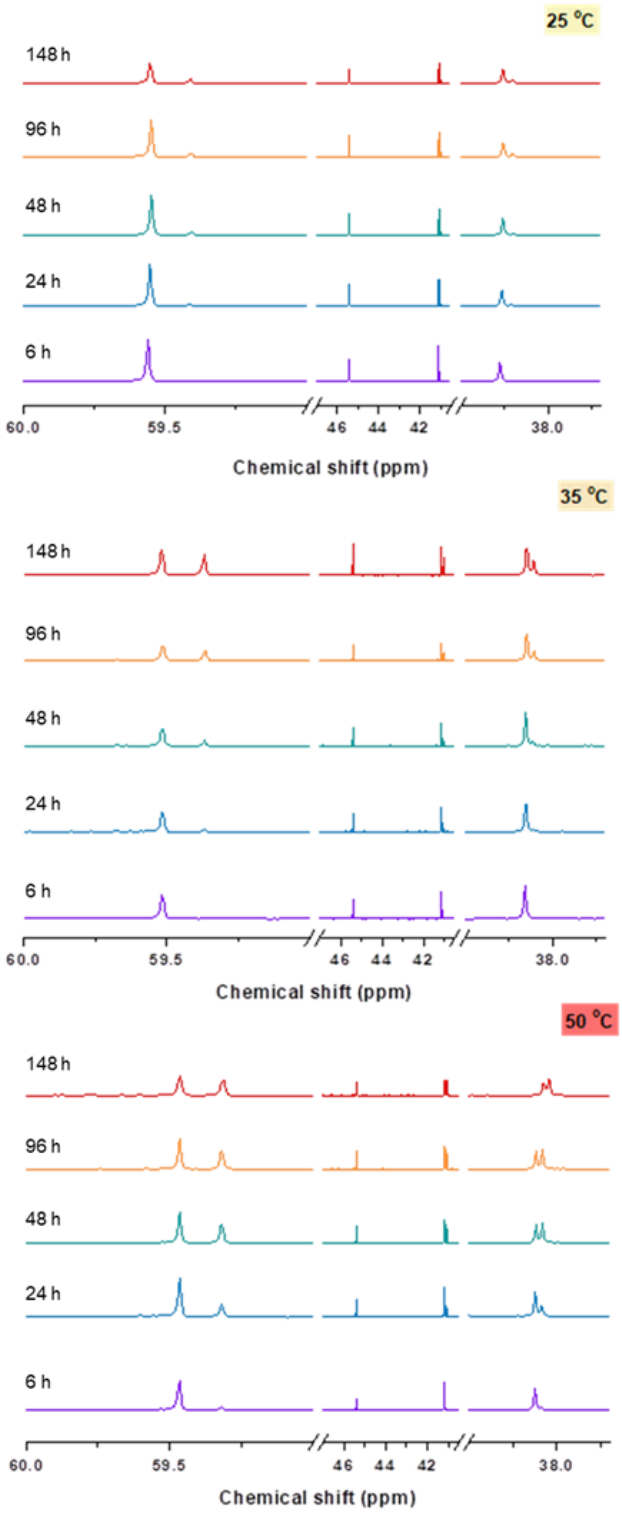

Figure S13. ^{13}C NMR spectrum of the aliphatic disulfide metathesis model reaction at different temperature of 25, 35, and 50 °C.

Supporting Note 2. Details of the Molecular Dynamics Simulations

The ability of self-healing polymers hinges upon factors such as H-bonding and the Bond Dissociation Energy of the S-S bond ($BDE_{S\text{-}S}$), as previously discussed. For a material to possess effective self-healing properties, reversible bond formation and breakage are crucial. Ideally, a multitude of H-bonds with short lifetimes is preferred. This is because excessively strong and long-lived H-bonds may restrict the reversibility of H-bonding formation and breakage.

With this understanding, we performed molecular dynamics simulations on two polymers, E-HD and C-HD, to gain insights into H-bonding interactions, and their quantity and lifespan. A linear chain comprising 10 repeating units of each polymer was constructed using the *Build*. The linear chain structure was optimized using the *Forcite* module, accounting for both electrostatic and van der Waals interactions via an atom-based approach. The *Smart* algorithm, a cascade of the steepest descent, adopted basis Newton-Raphson sets, and a quasi-Newton method, was utilized for rapid convergence. A cubic cell containing three polymer chains was optimized with the *Forcite* module. The optimized cell underwent relaxation through the following steps: The initial NPT annealing was conducted with an initial temperature of 300 K, an intermediate temperature of 600 K, and a pressure of 1 bar for 120 cycles. A second NPT annealing, identical to the first, followed, except with double the step cycles. After annealing, two NPT simulations were performed. The first NPT ran with a pressure of 1 bar and temperature of 300 K for 50 ps. The second NPT ran for 1 ns under the same conditions. An NVT simulation was executed for 5 ns at a pressure of 1 bar and a temperature of 300 K, and the final NPT ran for 3 ns.[29, 30] During the final NPT process, the standard deviation of density reached 0.006 g cm^{-3}, indicating the cells had achieved equilibrium. All time steps used in this study were 1 fs unless otherwise specified.

We calculated the number and lifetime of H-bonds for simulations running 850 ps with a time step of 0.1 ps. In the unit cell, H-bonds were identified by a distance of less than 2.5 Å between a hydrogen atom attached to electronegative atoms (like N and O) and another N or O that is not directly connected to H. We used a Perl-based script capable of identifying all H-bonds present in the unit cell for each frame based on distance, and computing their lengths.

All molecular dynamics simulations employed the COMPASS III forcefield to describe bonded and nonbonded interaction energy.[31] We computed the electrostatic interaction using the Ewald summation with an energy cutoff of 0.001 kcal/mol, while the nonelectrostatic interaction (van der Waals) was included using an atom-based summation method with a cutoff distance of 12.5 Å. BIOVIA Material Studio 6.0 was used for all molecular dynamics simulations.

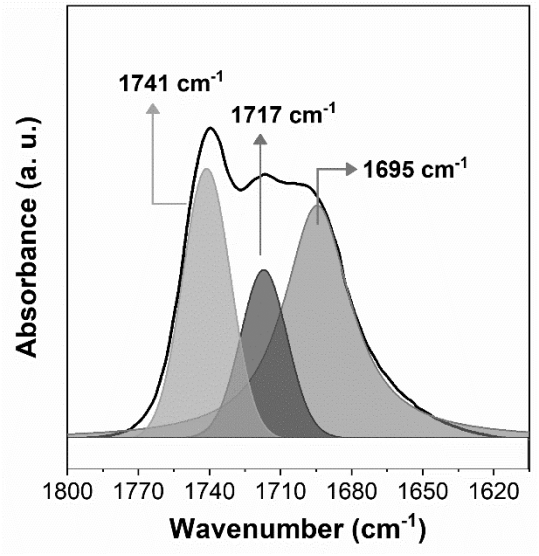

Figure S14. The carbonyl region of FTIR spectrum with peak deconvolution for C-HD.

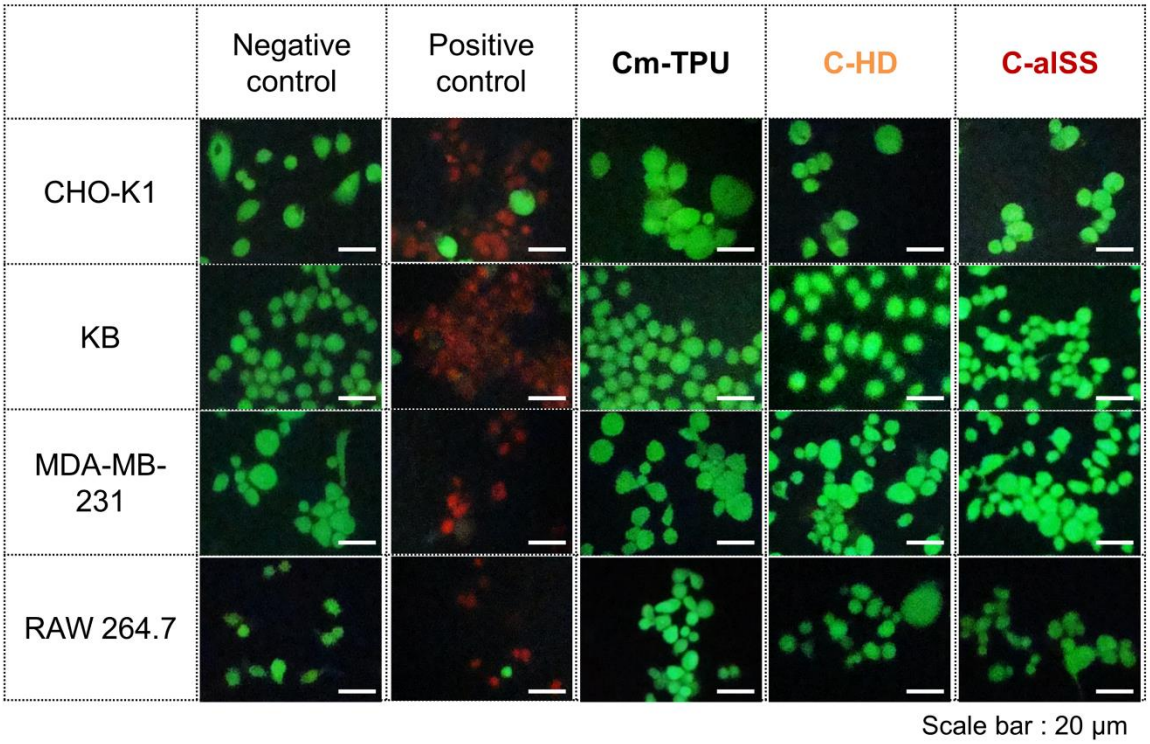

Figure S15. Confocal images of different types of cells treated with FDA/EB solution to identify live cells (green).

Movie S1. Manual handling and 1-kg weight-lifting test of chopped C-alSS film after healing at 25 °C.

Movie S2. Drop-ball (3-kg) test of C-alSS film (thickness: 0.5 mm); stabbing, healing at 35 °C for 6 h.

Movie S3. C-alSS film immersed in tap-water at 25 °C for 24 h.

Movie S4. C-alSS film immersed in boiling water for 0.5 h.

Movie S5. Colorless transparent C-alSS as a protective film on the mobile device demonstrating touch screen.

Movie S6. Three different films made of polypropylene (PP), polyethylene terephthalate (PET), and C-alSS were scratched with a copper brush

Movie S7. Stretching and releasing of dumbbell-shaped specimens of the synthesized TPUs.

Movie S8. Tensile experiment of C-alSS specimen of cut and healed at 35 °C for 6 h; stretched up to 400%.

Supporting References

1. J. M. Matxain, J. M. Asua and F. Ruipérez, *Phys. Chem. Chem. Phys.*, 2016, **18**, 1758-1770.
2. Y. Shao, Z. Gan, E. Epifanovsky, A. T. B. Gilbert, M. Wormit, J. Kussmann, A. W. Lange, A. Behn, J. Deng, X. Feng, D. Ghosh, M. Goldey, P. R. Horn, L. D. Jacobson, I. Kaliman, R. Z. Khaliullin, T. Kuś, A. Landau, J. Liu, E. I. Proynov, Y. M. Rhee, R. M. Richard, M. A. Rohrdanz, R. P. Steele, E. J. Sundstrom, H. L. Woodcock, P. M. Zimmerman, D. Zuev, B. Albrecht, E. Alguire, B. Austin, G. J. O. Beran, Y. A. Bernard, E. Berquist, K. Brandhorst, K. B. Bravaya, S. T. Brown, D. Casanova, C.-M. Chang, Y. Chen, S. H. Chien, K. D. Closser, D. L. Crittenden, M. Diedenhofen, R. A. DiStasio, H. Do, A. D. Dutoi, R. G. Edgar, S. Fatehi, L. Fusti-Molnar, A. Ghysels, A. Golubeva-Zadorozhnaya, J. Gomes, M. W. D. Hanson-Heine, P. H. P. Harbach, A. W. Hauser, E. G. Hohenstein, Z. C. Holden, T.-C. Jagau, H. Ji, B. Kaduk, K. Khistyaev, J. Kim, J. Kim, R. A. King, P. Klunzinger, D. Kosenkov, T. Kowalczyk, C. M. Krauter, K. U. Lao, A. D. Laurent, K. V. Lawler, S. V. Levchenko, C. Y. Lin, F. Liu, E. Livshits, R. C. Lochan, A. Luenser, P. Manohar, S. F. Manzer, S.-P. Mao, N. Mardirossian, A. V. Marenich, S. A. Maurer, N. J. Mayhall, E. Neuscamman, C. M. Oana, R. Olivares-Amaya, D. P. O′Neill, J. A. Parkhill, T. M. Perrine, R. Peverati, A. Prociuk, D. R. Rehn, E. Rosta, N. J. Russ, S. M. Sharada, S. Sharma, D. W. Small, A. Sodt, T. Stein, D. Stück, Y.-C. Su, A. J. W. Thom, T. Tsuchimochi, V. Vanovschi, L. Vogt, O. Vydrov, T. Wang, M. A. Watson, J. Wenzel, A. White, C. F. Williams, J. Yang, S. Yeganeh, S. R. Yost, Z.-Q. You, I. Y. Zhang, X. Zhang, Y. Zhao, B. R. Brooks, G. K. L. Chan, D. M. Chipman, C. J. Cramer, W. A. Goddard, M. S. Gordon, W. J. Hehre, A. Klamt, H. F. Schaefer, M. W. Schmidt, C. D. Sherrill, D. G. Truhlar, A. Warshel, X. Xu, A. Aspuru-Guzik, R. Baer, A. T. Bell, N. A. Besley, J.-D. Chai, A. Dreuw, B. D. Dunietz, T. R. Furlani, S. R. Gwaltney, C.-P. Hsu, Y. Jung, J. Kong, D. S. Lambrecht, W. Liang, C. Ochsenfeld, V. A. Rassolov, L. V. Slipchenko, J. E. Subotnik, T. Van Voorhis, J. M. Herbert, A. I. Krylov, P. M. W. Gill and M. Head-Gordon, *Mol. Phys.*, 2015, **113**, 184-215.
3. W. Kong, Y. Yang, Y. Wang, H. Cheng, P. Yan, L. Huang, J. Ning, F. Zeng, X. Cai and M. Wang, *J. Mater. Chem. A*, 2022, **10**, 2012-2020.
4. J. Hu, R. Mo, X. Jiang, X. Sheng and X. Zhang, *Polymer*, 2019, **183**, 121912.
5. M. Liu, J. Zhong, Z. Li, J. Rong, K. Yang, J. Zhou, L. Shen, F. Gao, X. Huang and H. He, *Eur. Polym. J.*, 2020, **124**, 109475.
6. J. Rong, J. Zhong, W. Yan, M. Liu, Y. Zhang, Y. Qiao, C. Fu, F. Gao, L. Shen and H. He, *Polymer*, 2021, **221**, 123625.
7. Y. Xu and D. Chen, *Macromol. Chem. Phys.*, 2016, **217**, 1191-1196.
8. X. Wang, H. Zhang, B. Yang, L. Wang and H. Sun, *New J. Chem.*, 2020, **44**, 5746-5754.
9. H. Jia and S.-Y. Gu, *J. Polym. Res.*, 2020, **27**, 298.
10. J. Dong, B. Liu, H. Ding, J. Shi, N. Liu, B. Dai and I. Kim, *Polym. Chem.*, 2020, **11**, 7524-7532.
11. F. Dong, X. Yang, L. Guo, Y. Wang, H. Shaghaleh, Z. Huang, X. Xu, S. Wang and H. Liu, *J. Mater. Chem. A*, 2022, **10**, 10139-10149.
12. Y.-m. Ha, Y.-O. Kim, S. Ahn, S.-k. Lee, J.-s. Lee, M. Park, J. W. Chung and Y. C. Jung, *Eur. Polym. J.*, 2019, **118**, 36-44.
13. Y. Lai, X. Kuang, P. Zhu, M. Huang, X. Dong and D. Wang, *Adv. Mater.*, 2018, **30**, 1802556.

14. W. Ussama and M. Shibata, *J. Polym. Res.*, 2021, **28**, 5.
15. G. Ye and T. Jiang, *Polymers*, 2021, **13**.
16. Z. Q. Lei, H. P. Xiang, Y. J. Yuan, M. Z. Rong and M. Q. Zhang, *Chem. Mater.*, 2014, **26**, 2038-2046.
17. S. Sarkar, S. L. Banerjee and N. K. Singha, *Macromol. Mater. Eng.*, 2021, **306**, 2000626.
18. H. Wu, X. Liu, D. Sheng, Y. Zhou, S. Xu, H. Xie, X. Tian, Y. Sun, B. Shi and Y. Yang, *Polymer*, 2021, **214**, 123261.
19. L. Zhang, T. Qiu, X. Sun, L. Guo, L. He, J. Ye and X. Li, *Polymers*, 2020, **12**.
20. Y. Eom, S.-M. Kim, M. Lee, H. Jeon, J. Park, E. S. Lee, S. Y. Hwang, J. Park and D. X. Oh, *Nat. Commun.*, 2021, **12**, 621.
21. S.-M. Kim, H. Jeon, S.-H. Shin, S.-A. Park, J. Jegal, S. Y. Hwang, D. X. Oh and J. Park, *Adv. Mater.*, 2018, **30**, 1705145.
22. C. Liu, Q. Yin, Q. Yuan, L. Hao, L. Shi, Y. Bao, B. Lyu and J. Ma, *Polym. Chem.*, 2022, **13**, 5647-5658.
23. T. Jing, X. Heng, T. Jingqing, L. Haozhe, L. Li, L. Pingyun and G. Xiaode, *Polymer*, 2023, **265**, 125590.
24. T. Jing, X. Heng, X. Guifeng, L. Li, P. Li and X. Guo, *Mater. Chem. Front.*, 2022, **6**, 1161-1171.
25. J. He, F. Song, X. Li, L. Chen, X. Gong and W. Tu, *J. Polym. Res.*, 2021, **28**, 122.
26. R. H. Aguirresarobe, L. Martin, M. J. Fernandez-Berridi and L. Irusta, *Express Polym. Lett.*, 2017, **11**, 266-277.
27. A. Rekondo, R. Martin, A. Ruiz de Luzuriaga, G. Cabañero, H. J. Grande and I. Odriozola, *Mater. Horiz.*, 2014, **1**, 237-240.
28. L. Yang, L. Sun, H. Huang, W. Zhu, Y. Wang, Z. Wu, R. E. Neisiany, S. Gu and Z. You, *Adv. Sci.*, 2023, **10**, 2207527.
29. H. C. Andersen, *J. Chem. Phys.*, 1980, **72**, 2384-2393.
30. G. J. Martyna, D. J. Tobias and M. L. Klein, *J. Chem. Phys.*, 1994, **101**, 4177-4189.
31. R. L. C. Akkermans, N. A. Spenley and S. H. Robertson, *Mol. Simulat.*, 2021, **47**, 540-551.